Supplemental Figure Legends

Figure S1. The binding activity of cross-reactive antibodies against MERS-CoV and human common-cold CoVs.

The neutralization activity of four broadly neutralizing antibodies against SARS-CoV-2 NTD, MERS-CoV spike, HCoV-OC43 spike, HCoV-NL63, and HCoV-229E shown for (A) DH1235, (B) DH1073, (C) DH1046, and (D) DH1047.

Figure S2. NSEM of DH1047 bound to bat RsSHC014 and SARS-CoV spike ectodomains.

(A) Representative 2D class averages of bat RsSHC014 2P spike ectodomain bound to DH1047 Fab.

(B) Overlay of 3D reconstruction of DH1047 bound to bat RsSHC014 2P (grey) and SARS-CoV-2 HexaPro (purple) S ectodomains.

(C) Representative 2D class averages of SARS-CoV 2P spike ectodomain bound to DH1047 Fab

(D) Overlay of 3D reconstruction of DH1047 bound to bat SARS-CoV 2P (grey) and SARS-CoV-2 HexaPro (purple) S ectodomains. The red boxes in panels A and C indicate the classes that show DH1047 Fab bound to spike.

Figure S3. Lung H+E staining of SARS-CoV infected mice.

Pathologic features of acute lung injury were scored using two separate tools: the American Thoracic Society Lung Injury Scoring (ATS ALI) system. Using this ATS ALI system, we created an aggregate score for the following features: neutrophils in the alveolar and interstitial space, hyaline membranes, proteinaceous debris filling the air spaces, and alveolar septal thickening. Three randomly chosen high power (×60) fields of diseased lung were assessed per mouse. Representative images are shown from vehicle and RDV-treated mice. All images were taken at the same magnification. The black bar indicates 100 μm scale. (A) CH65 control prophylaxis. (B) CH65 therapy. (C) DH1047 prophylaxis. (D) DH1047 therapy.

Figure S4. The affinity data of DH1047 against SARS-CoV and RsSHC014 spikes.

Surface plasmon resonance (SPR) binding experiments of DH1047 against (A) SARS-CoV-2 Toronto and (B) RsSHC014. Binding affinity measurements are shown in the tables and response

781 units (RU) as a function of time in seconds (s) is shown for both SARS-CoV and RsSHC014.
782 SPR experiments were repeated twice.
783
784 **Figure S5. Cryo-EM data processing for the SARS-CoV spike ectodomain bound to**
785 **DH1047, Related to Figure 2.**
786 (A) Representative cryo-EM micrograph.
787 (B) Cryo-EM CTF fit.
788 (C) Representative 2D class averages from Cryo-EM dataset.
789 (D) *Ab initio* reconstruction.
790 (E) Refined map.
791 (F) Fourier shell correlation curve.
792 (G) Refined cryo-EM map colored by local resolution.
793 (H) Zoom-in images showing the SD1, NTD, HR1/CH and RBD/Fab contact regions in the
794 structure. The cryo-EM map is shown as a blue mesh and the fitted model is in cartoon
795 representation, with residues shown as stick.
796
797 **Figure S6. DH1047 and ADG-2 binds the RBD of SARS-Cov and SARS-CoV-2 spike**
798 **ectodomains using a similar footprint.**
799 (A) Cartoon representation of DH1047 (colored in pale green) bound to the RBD (grey surface,
800 ACE2 binding site in yellow) of SARS-CoV S ectodomain and ADG-2 (cyan) bound to SARS-
801 CoV-2 S ectodomain. The homologous Fab ADI-19425 (PDB 6APC) was docked in the ADG-2
802 cryo-EM map (EMD-23160) to generate the model.

(B) DH1047 and ADG-2 bind partially overlapping binding sites on the RBD.

Supplemental Table 1: monoclonal antibody screen against SARS-CoV-2 2AA MA, SARS-CoV, WIV-1, and RsSHC014

Supplemental Table 2: Immunogenetic characteristics of broadly cross-reactive mAbs.

826

827

828

829

830

Supplementary Table 3. Cryo-EM data collection and refinements statistics.

PDB ID	
EMDB ID	
Data collection and processing	
Microscope	FEI Titan Krios
Detector	Gatan K3
Magnification	81,000
Voltage (kV)	300
Electron exposure (e–/A□2)	54.1
Defocus range (μm)	~0.75-2.50
Pixel size (A□)	1.08
Reconstruction software	cryoSparc
Symmetry imposed	C1
Initial particle images (no.)	2,370,616
Final particle images (no.)	284,619
Map resolution (A□)	3.43
FSC threshold	0.143
Refinement	
Initial model used	7LD1
Model resolution (A□)	3.43
FSC threshold	0.143
Model composition	
Nonhydrogen atoms	28,048
Protein residues	3,737
R.m.s. deviations	
Bond lengths (A□)	0.016
Bond angles (°)	1.956
Validation	
MolProbity score	1.79
Clashscore	1.65
Poor rotamers (%)	2.36

EM ringer score	2.9	831
Ramachandran plot		
Favored (%)	88.54	832
Allowed (%)	9.79	833
Disallowed (%)	1.66	
		834

835

Figure S1

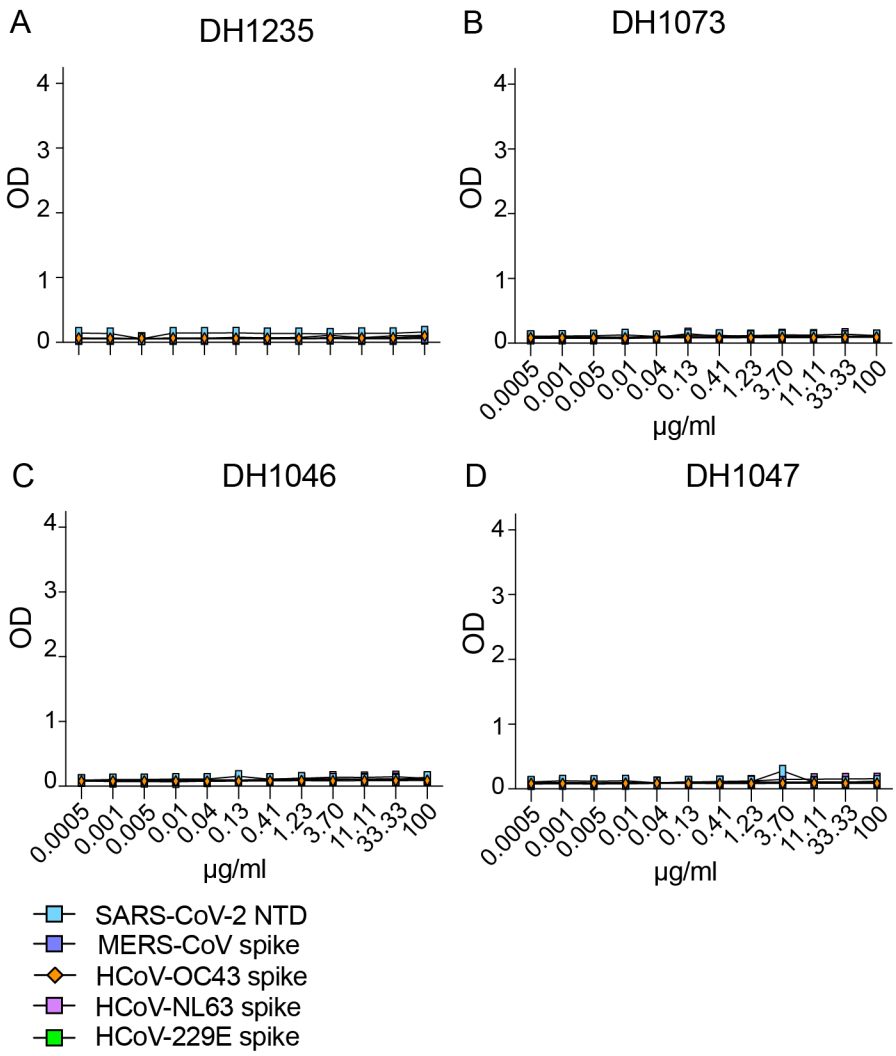

Figure S2

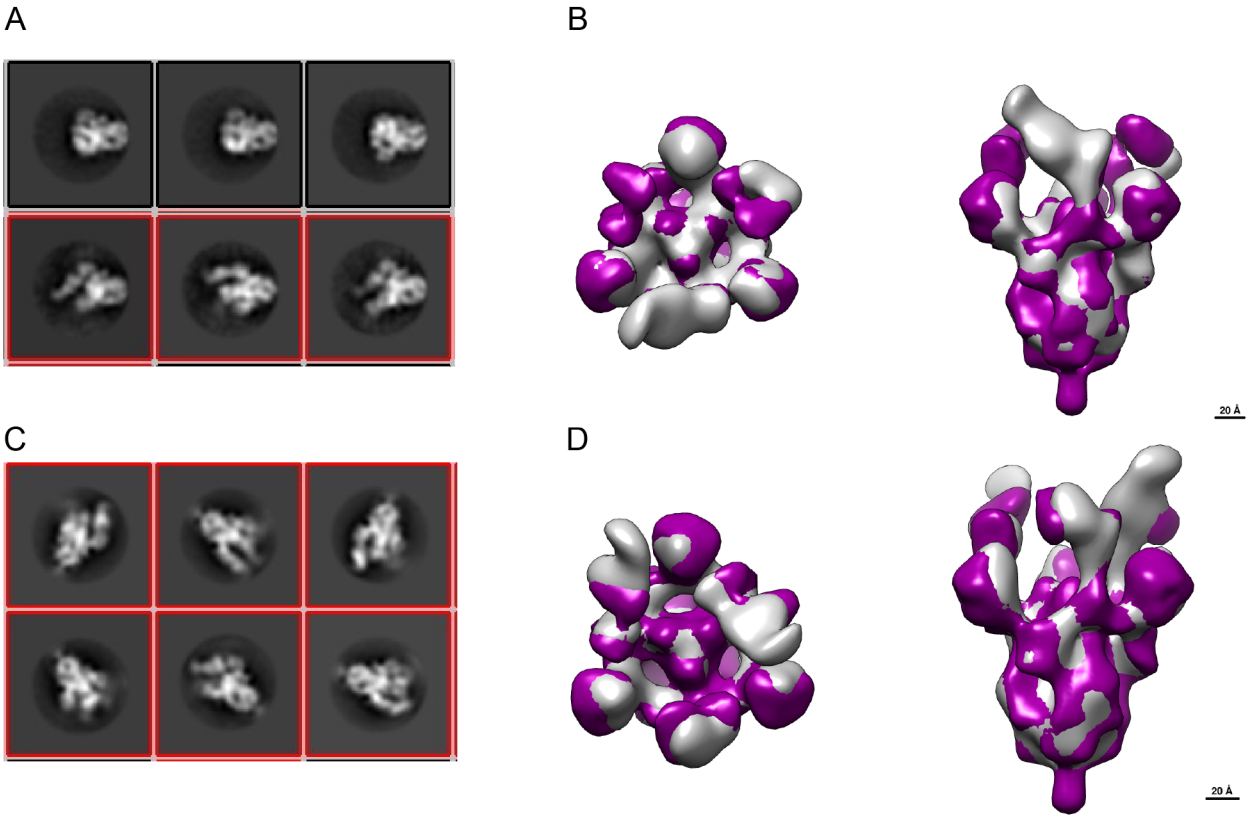

Figure S3

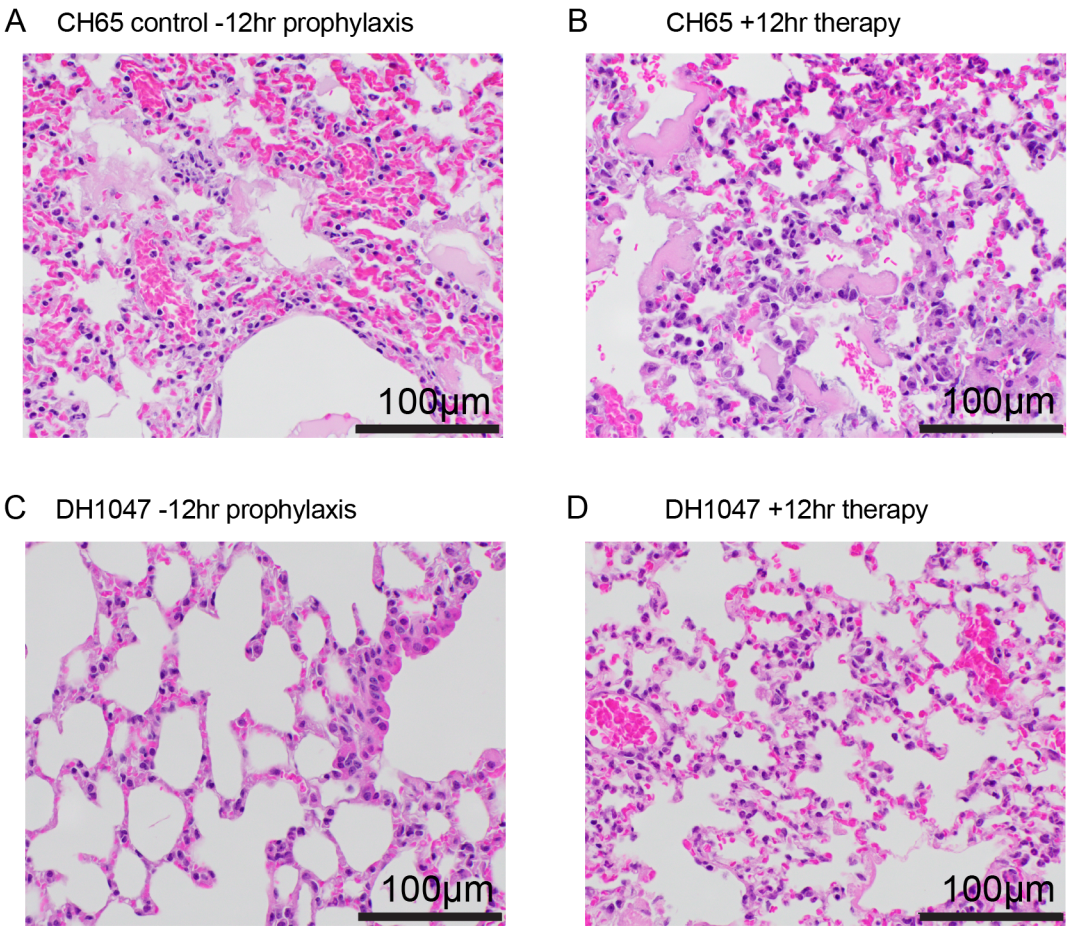

Figure S4

A

SARS-CoV Toronto spike			
Fab	ka (1/Ms)	kd (1/s)	KD(nM)
DH1047	9.622E+4	<1.0E-5	<0.1

B

RsSCH014 spike			
Fab	ka (1/Ms)	kd (1/s)	KD(nM)
DH1047	8.602E+4	<1.0E-5	<0.1

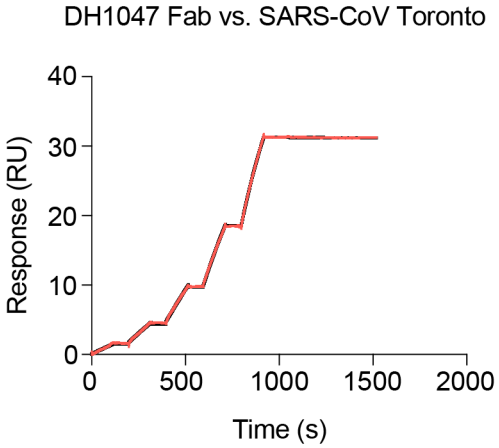

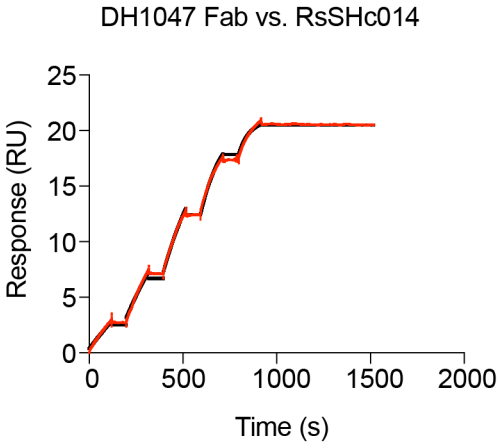

Figure S5

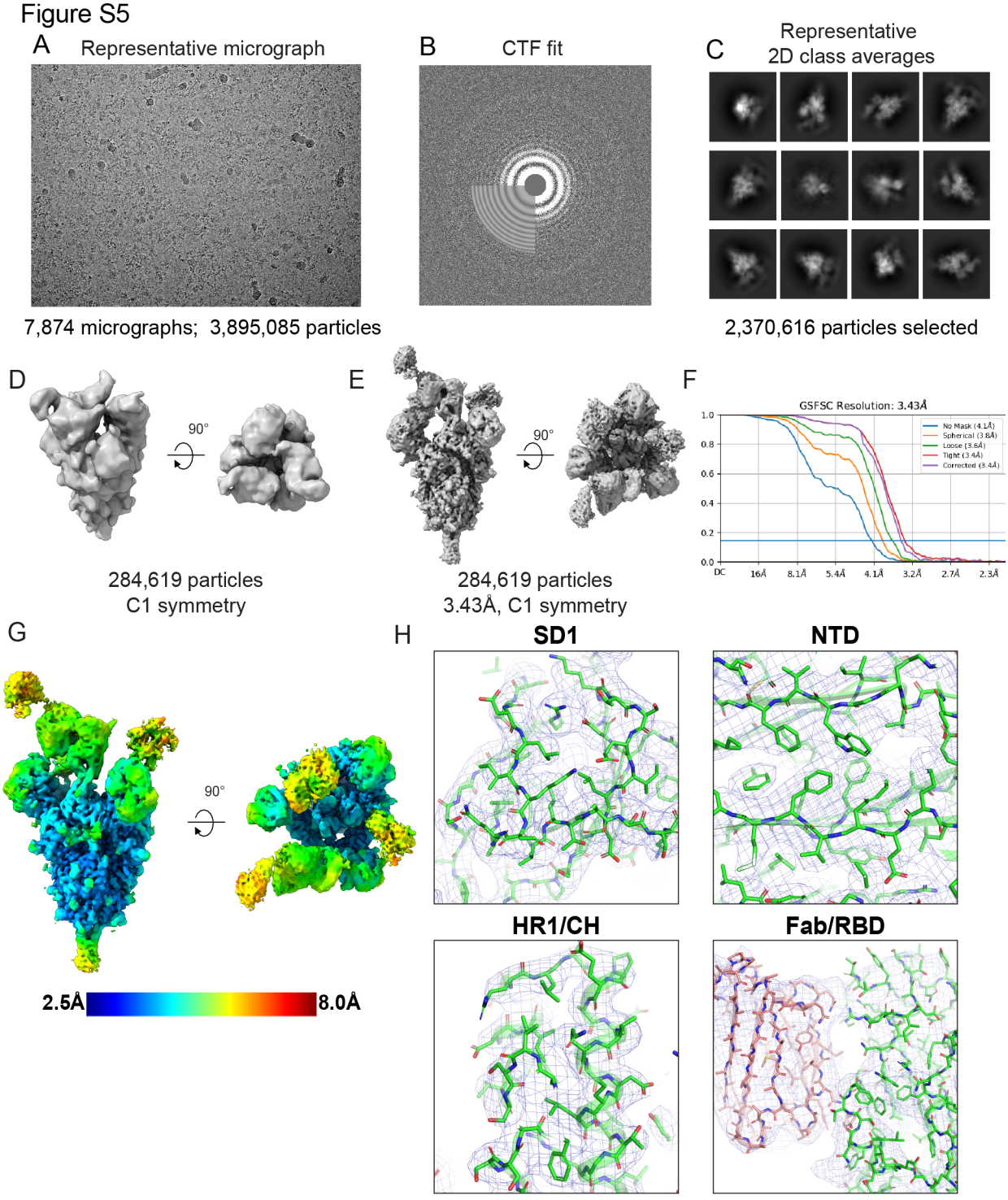

Figure S6

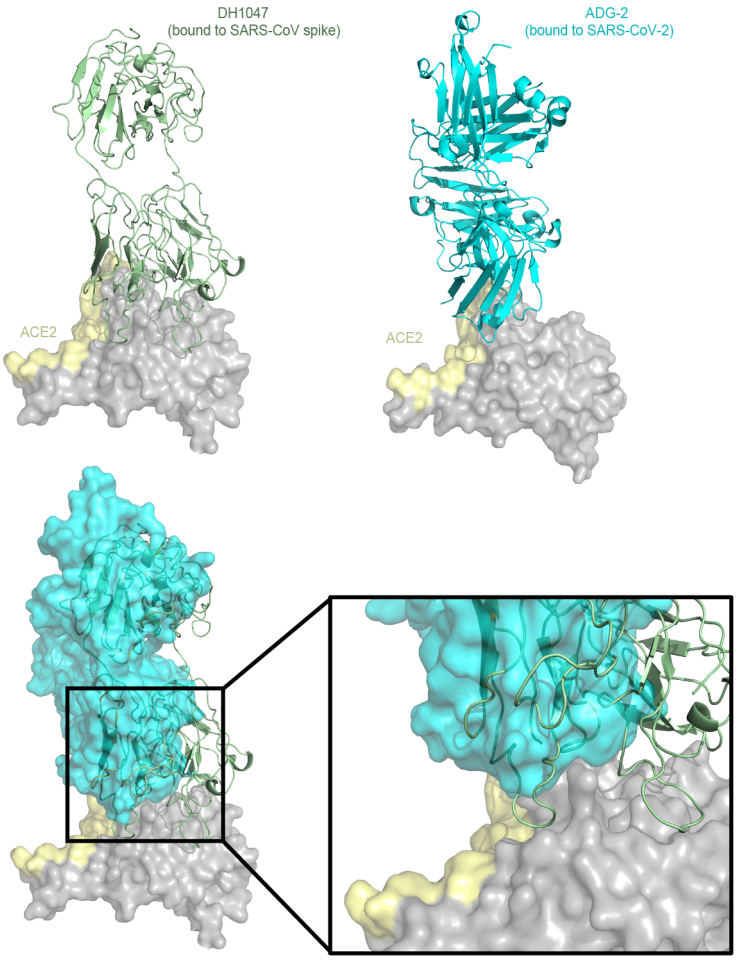

Supplemental Table 1: monoclonal antibody screen against SARS-CoV-2 2AA MA, SARS-CoV, WIV-1, and RsSHC014

mAb #	DH #	mAb	Specificity to SARS-CoV-2	ELISA cross-reactivity	Live virus neutralization IC_{50} (μg/ml)			
					SARS-CoV-2 2AA MA	SARS-CoV	WIV-1	RsSHC014
1	DH1058	Ab711725_G1.4A/293i/Citrate	S2	SARS-CoV-1, MERS-CoV, 229E, NL63, HKU1, OC43	>10	>10	>10	>10
2	DH1057	Ab025934_G1.4A/293i/Citrate	S2	SARS-CoV-1, OC43	>10	>10	>10	>10
18	**DH1047**	**Ab712384_LS/293i/Citrate**	**RBD**	**SARS-CoV, SARS-CoV-2, and bat CoVs**	**0.3979**	**0.0287**	**0.191**	**0.2005**
45	DH1203	Ab026044_LS/293i/Citrate	RBD	SARS-CoV and SARS-CoV-2	3.768	0.04781	>10	>10
46	DH1127	Ab026075_LS/293i/Citrate	RBD	SARS-CoV and SARS-CoV-2	>10	>10	>10	>10
47	DH1059	Ab026129L2_LS/293i/Citrate	no binding	SARS-CoV-2	>10	>10	>10	>10
48	DH1081	Ab026147_LS/293i/Citrate	NTD	SARS-CoV and SARS-CoV-2	>10	>10	>10	>10
49	DH1085	Ab026160_LS/293i/Citrate	no binding	SARS-CoV-2	>10	>10	>10	>10
50	DH1080	Ab026162_LS/293i/Citrate	RBD	SARS-CoV and SARS-CoV-2	>10	0.0059	0.0330	>10
51	DH1061.1	Ab026164_LS/293i/Citrate	NTD	SARS-CoV and SARS-CoV-2	>10	>10	>10	>10
52	DH1065	Ab026172_LS/293i/Citrate	NTD	SARS-CoV and SARS-CoV-2	>10	>10	>10	>10
53	DH1066	Ab026186_LS/293i/Citrate	NTD	only SARS-CoV	>10	>10	>10	>10
54	DH1064	Ab026188_LS/293i/Citrate	RBD	SARS-CoV and SARS-CoV-2	>10	0.0216	>10	>10
55	DH1067	Ab026196_LS/293i/Citrate	NTD	SARS-CoV and SARS-CoV-2	>10	>10	>10	>10
56	DH1069	Ab026200_LS/293i/Citrate	NTD	SARS-CoV and SARS-CoV-2	>10	>10	>10	>10
57	**DH1046**	**Ab026204_LS/293i/Citrate**	**RBD**	**SARS-CoV, SARS-CoV-2, and bat CoVs**	**2.857**	**0.1033**	**0.4248**	**1.274**
58	DH1068	Ab026217_LS/293i/Citrate	NTD	SARS-CoV and SARS-CoV-2	>10	>10	>10	>10
59	DH1086	Ab026240_LS/293i/Citrate	NTD	SARS-CoV and SARS-CoV-2	>10	>10	>10	>10
60	DH1071	Ab026243_LS/293i/Citrate	NTD	SARS-CoV and SARS-CoV-2	>10	>10	>10	>10
61	DH1088	Ab026245_LS/293i/Citrate	no binding	SARS-CoV-2	>10	>10	>10	>10
62	**DH1073**	**Ab026258_LS/293i/Citrate**	**RBD**	**SARS-CoV, SARS-CoV-2, and bat CoVs**	**0.8088**	**0.0161**	**0.267**	**>10**
64	**DH1235**	**Ab026319_LS/293i/Citrate**	**RBD**	**SARS-CoV, SARS-CoV-2, and bat CoVs**	**0.1226**	**0.0403**	**0.0602**	**>10**
65	#N/A	Ab026336_LS/293i/Citrate	RBD	SARS-CoV and SARS-CoV-2	>10	>10	>10	>10
66	DH1193	Ab712053_LS/293i/Citrate	RBD	SARS-CoV and SARS-CoV-2	4.345	>10	>10	>10
67	DH1152	Ab712109_LS/293i/Citrate	RBD	SARS-CoV and SARS-CoV-2	>10	>10	>10	>10
68	DH1171	Ab712113_LS/293i/Citrate	NTD	SARS-CoV and SARS-CoV-2	>10	>10	>10	>10
69	DH1109	Ab712156_LS/293i/Citrate	RBD	SARS-CoV and SARS-CoV-2	>10	>10	>10	>10
70	DH1208	Ab712166_LS/293i/Citrate	RBD	SARS-CoV and SARS-CoV-2	>10	>10	>10	>10
71	DH1166	Ab712215_LS/293i/Citrate	RBD	SARS-CoV and SARS-CoV-2	>10	>10	>10	>10
72	DH1191	Ab712224_LS/293i/Citrate	RBD	SARS-CoV and SARS-CoV-2	>10	>10	>10	>10
73	DH1120	Ab712294_LS/293i/Citrate	RBD	SARS-CoV and SARS-CoV-2	>10	>10	>10	>10
74	DH1110	Ab712312_LS/293i/Citrate	NTD	SARS-CoV and SARS-CoV-2	>10	>10	>10	>10
75	DH1106	Ab712366_LS/293i/Citrate	NTD	SARS-CoV and SARS-CoV-2	>10	>10	>10	>10
76	DH1112	Ab712370_LS/293i/Citrate	RBD	SARS-CoV and SARS-CoV-2	>10	0.0023	0.1617	>10
77	DH1117	Ab712376_LS/293i/Citrate	RBD	SARS-CoV and SARS-CoV-2	>10	>10	>10	>10
78	DH1115	Ab712378_LS/293i/Citrate	RBD	SARS-CoV and SARS-CoV-2	>10	0.0083	0.1614	>10
79	DH1093	Ab712381_LS/293i/Citrate	NTD	SARS-CoV and SARS-CoV-2	>10	>10	>10	>10
80	DH1095	Ab712402_LS/293i/Citrate	RBD	SARS-CoV	>10	>10	>10	>10
81	DH1113	Ab712404_LS/293i/Citrate	RBD	SARS-CoV and SARS-CoV-2	>10	>10	>10	>10
82	DH1114	Ab712407_LS/293i/Citrate	NTD	SARS-CoV and SARS-CoV-2	>10	>10	>10	>10
84	DH1098	Ab712416_LS/293i/Citrate	RBD	SARS-CoV and SARS-CoV-2	>10	0.0052	0.0318	>10
85	DH1101	Ab712423_LS/293i/Citrate	RBD	SARS-CoV and SARS-CoV-2	>10	0.0012	>10	>10
86	#N/A	Ab712561_LS/293i/Citrate	RBD	SARS-CoV and SARS-CoV-2	>10	0.0399	0.4312	>10
87	#N/A	Ab712572_LS/293i/Citrate	RBD	SARS-CoV and SARS-CoV-2	>10	>10	>10	>10
88	#N/A	Ab712584_LS./293i/Citrate	RBD	SARS-CoV and SARS-CoV-2	>10	>10	>10	>10
89	#N/A	Ab712585_LS./293i/Citrate	RBD	SARS-CoV and SARS-CoV-2	>10	>10	>10	>10
90	#N/A	Ab712588_LS./293i/Citrate	RBD	SARS-CoV and SARS-CoV-2	>10	>10	>10	>10
91	#N/A	Ab712614L_LS/293i/Citrate	RBD	SARS-CoV and SARS-CoV-2	>10	>10	>10	>10
92	#N/A	Ab712617_LS/293i/Citrate	RBD	SARS-CoV and SARS-CoV-2	>10	>10	>10	>10
93	#N/A	Ab712618_LS/293i/Citrate	RBD	SARS-CoV and SARS-CoV-2	9.877	>10	>10	>10

Supplemental Table 2: Immunogenetic characteristics of broadly cross-reactive mAbs

DH#	Antibody ID	Binding Specificity	Cross Reactivity	Antibody Gene Analysis									
				Donor ID	Time Piont	HCDR3 Length	Heavy chain mutation	VH_Gene	JH_Gene	LCDR3 Length	Light chain mutation	VL_Gene	JL_Gene
DH1235	Ab026319_LS	RBD	SARS-CoV-1	SARS-CoV-2 convalescent	Day 36	21	1.68	IGHV3-48	IGHJ4	9	1.75	IGLV4-60	IGLJ2
DH1073	Ab026258_LS	RBD	SARS-CoV-1	SARS-CoV convalescent	Year 17	15	9.06	IGHV1-46	IGHJ6	11	2.92	IGKV3-11	IGKJ1
DH1046	Ab026204_LS	RBD	SARS-CoV, PCoV GXP4L, Bat CoV RsSHC014, Bat CoV RaTG13	SARS-CoV convalescent	Year 17	24	4.70	IGHV3-23	IGHJ6	9	3.65	IGKV1-5	IGKJ2
DH1047	Ab712384_LS	RBD	SARS-CoV, PCoV GXP4L, Bat CoV RsSHC014, Bat CoV RaTG13	SARS-CoV convalescent	Year 17	24	8.05	IGHV1-46	IGHJ4	9	2.05	IGKV4-1	IGKJ1